



High density sulfonated magnetic carbon quantum dots as a photo enhanced, photo-induced proton generation, and photo switchable solid acid catalyst for room temperature one-pot reaction

Negin Sarmasti¹ · Ardeshir Khazaei¹ · Jaber Yousefi Seyf²

Received: 29 December 2018 / Accepted: 8 April 2019
© Springer Nature B.V. 2019

Abstract

The preparation of photo enhanced and switchable (on/off mode) sulfonated magnetic carbon quantum dots was investigated in the present work. First, the as-synthesized carbon quantum dots (CQDs) were easily separated using a magnet (instead of using a dialysis method), then CQDs decorated with high density (9.6 mmol/g) acid groups (sulfonic + carboxylic) using chlorosulfonic acid. The photo-switchable activity of the catalyst related to the photoexcitation of charge separation which in turn leads to electron withdrawing property in sulfonic groups. On the other hand, it was shown that sulfonated magnetic carbon quantum dot (S-M-CQDs) is more efficient than magnetic carbon quantum dot (M-CQDs). The as-prepared catalyst was characterized using SEM, TEM, EDX, XRD, IR, VSM and TGA. The catalytic activity of the as-prepared catalyst was evaluated at room temperature in one-pot reaction (synthesis of hexahydroquinoline derivatives). The as-synthesized catalyst easily retrieved using a magnet (than ultracentrifugation) and used in the next cycles.

Keywords Photocatalysis · Quantum dots · One-pot reaction · Chlorosulfonic acid · Nano Fe₃O₄

Electronic supplementary material The online version of this article (<https://doi.org/10.1007/s11164-019-03829-w>) contains supplementary material, which is available to authorized users.

✉ Ardeshir Khazaei
khazaei_1326@yahoo.com

¹ Faculty of Chemistry, Bu-Ali Sina University, Hamedan 6517838683, Iran

² Department of Chemical Engineering, Hamedan University of Technology, Hamedan, Iran

Introduction

Carbon has a broad family of allotropes which includes diamond, graphite, fullerene, carbon nanotubes, single-walled carbon nanohorns (SWNHs), onion-like carbon (OLC) spheres, bamboo-like nanotubes, graphene, graphene dots and carbon dots. Diamond and graphite are the oldest and most known allotropes. C_{60} , which is known as fullerene is the first carbon nanostructure, which was initially reported in 1985 [1, 2], and 6 years later (in 1991) carbon nanotubes (CNTs) were discovered by Iijima [3, 4]. In sequence, other carbon nanostructures with unique shapes such as single-walled carbon nanohorns (SWNHs), onion-like carbon (OLC) spheres, and bamboo-like nanotubes were discovered. The graphene as the building block of graphite was first isolated and characterized in 2004 by Novoselov et al. [5]. Graphene quantum dots (GQDs) with a dimension of a few nanometers with crystalline structure are defined as small pieces of graphene monolayer [6]. Finally, in 2004 carbon dots (C-dots) were identified during preparative gel electrophoresis purification of single wall carbon nanotubes (SWNTs), which was generated by the arc-discharge method [7]. Due to CQDs strong fluorescence property, they have recently attracted the attention of researchers. Accordingly, several methods have been developed for the synthesis of C-dots which can be categorized into two main categories, including chemical and physical methods [8]. Physical methods include arc-discharge [7], laser ablation/passivation [9], and plasma treatment [10]. Chemical methods include the electrochemical synthesis, combustion/thermal/hydrothermal/acidic oxidation, supported synthesis, microwave/ultrasonic, solution chemistry methods, cage-opening of fullerene, and etc. [11]. C-dots have also been prepared from candle soot following by acid treatments [12]. Because of strong and tunable photoluminescence (PL), C-dots have found important and wide applications in chemical sensing, bio-sensing, bioimaging, nanomedicine, photocatalysis and electrocatalysis [13]. However, few studies have focused on exploring the surface functionality of CQDs as catalytic sites in organic transformations. Carbon quantum dots and sulfonated carbon quantum dots (through concentrated H_2SO_4) have been used for Aldol condensations [14, 15], quinazolinone derivatives and aza-Michael adducts [16], esterification [15], Beckmann rearrangement [15] and ring opening reaction [17]. Purification of C-dots is achieved through a combination of un-commercial methods, including ultracentrifugation, filtration, dialysis, and column chromatography or gel electrophoresis. On the other hand, ultracentrifugation is used for separation of C-dots from reaction media, which is not an effective and economical method [14, 17].

With regards to the mentioned issues, in the present work, C-dots were prepared from candle soot, but magnetic nano- Fe_3O_4 was used for easy separation of carbon quantum dots (CQDs). In addition, rapid sulfonation of magnetic C-dots (M-CQDs) was achieved through chlorosulfonic acid than concentrated H_2SO_4 [17] (S-M-CQDs). We demonstrate that S-M-CQDs and M-CQDs act as photo switchable solid acid catalysts, which can catalyze the one-pot reactions (e.g. hexahydroquinoline derivatives) under UV irradiation and dark at room temperature. Finally the as-synthesized catalyst magnetically was recovered from the reaction media, and used in the next cycles.

Experimental

Reagents and characterization

Ferric chloride hexahydrate ($\text{FeCl}_3 \cdot 6\text{H}_2\text{O}$), ammonia (28% by weight), ferrous chloride tetrahydrate ($\text{FeCl}_2 \cdot 4\text{H}_2\text{O}$), phthalhydrazide, different aldehydes, dime-done, ethanol, chloroform, acetone, and chlorosulfonic acid were prepared from Merck company. The reaction progress was monitored using thin layer chromatography (TLC) (silica gel SIL G/UV 254 plates). Perkin Elmer PE-1600-FTIR was used to determine the Infrared spectra of products. Thermal gravimetric analysis (TGA) of the catalyst under a nitrogen atmosphere was used to determine the stability of the as-prepared catalyst. The Field emission scanning electron microscopy (FESEM), and Transmission electron microscopy (TEM) images were recorded with SIGMA VP-500 (ZEISS), Zeiss-EM10C-100 kV, respectively. Elemental analysis was measured using Energy dispersive X-ray analysis (EDXA) (Oxford Instrument). Vibrating sample magnetometer (VSM), model (MDKB), was used to determine the magnetic property of the as-catalyst.

Synthesis of the catalyst

Synthesis of Fe_3O_4 nanoparticles

The co-precipitation approach was used to synthesize the magnetic (Fe_3O_4) nanoparticles. First 11.3 g $\text{FeCl}_3 \cdot 6\text{H}_2\text{O}$ and 5.6 g $\text{FeCl}_2 \cdot 4\text{H}_2\text{O}$ was dissolved in deionized water at the 80 °C (600 rpm). After complete dissolution of the $\text{FeCl}_3 \cdot 6\text{H}_2\text{O}$ and $\text{FeCl}_2 \cdot 4\text{H}_2\text{O}$ in water, 25 ml ammonia (28% by weight) was added at once to the solution. The resulting black solution was vigorously stirred for 2 h at 80 °C under N_2 atmosphere. Then the precipitated magnetic nanoparticles were separated from the solution using a magnet. Nanoparticles were washed several times with water and then with acetone. Finally, a stable black magnetic dispersion was obtained which was dried in an oven.

Preparation of C-dot nanoparticles from candle soot

The soot was collected by placing an aluminum foil over the flame of a candle [12]. The particles in the soot agglomerated, so that micro-particles are formed. In order to uniform dispersion of C-dot nanoparticles in water, the acid treatment was used, so that 1 g soot was reflux in 16 M HNO_3 for 24 h. After cooling the reflux media up to room temperature, it was centrifuged (4000 rpm), which results in a brown solution and a black precipitation. The brown solution decanted and neutralized with Na_2CO_3 until the pH 7 (mixture A).

Preparation of Fe₃O₄@C-dot nanoparticles

1 g of the previous synthesized Fe₃O₄ nanoparticles was dispersed (15 min using an ultrasonic bath) in mixture A, and was stirred for 24 h at room temperature. The Fe₃O₄@C-dot nanoparticles were separated using a super magnet and washed several times with deionized water, then dried in an oven.

Preparation of Fe₃O₄@C-dot@SO₃H nanoparticles

1 g Fe₃O₄@C-dot nanoparticles (previous step) was dispersed in dried dichloromethane (15 min using an ultrasonic bath) and transferred to a bath with 0 °C controlled temperature (mixture B). Then 1 ml chlorosulfonic acid was mixed with 10 ml dried dichloromethane, and then it was added dropwise to the mixture B. Then the solution stirred approximately for 15 min until the all gases exhausted from the solution. Then the mixture B was stirred for 24 h at room temperature. Finally, Fe₃O₄@C-dot@SiO₃H was separated using a magnet, washed several times with dried CH₂Cl₂ and then dried in an oven. The details of the C-dot nanoparticles synthesis is given in the literature, so that the HNO₃ was selected as the best oxidant.

Results and discussion

Catalyst characterization

Micrographs obtained from scanning electron microscopy (SEM), and transmission electron microscopy (TEM) of the S-M-CQDs and M-CQDs are represented in the Fig. 1. Figure 1a, b show the SEM and TEM images of M-CQDs, respectively. Figure 1c, d represent the SEM and TEM images of the S-M-CQDs, respectively. The hydrogen bonds between OSO₃H groups in S-M-CQDs lead to agglomeration of nanoparticles, which can be seen in Fig. 1c, d. TEM images show that M-CQDs and S-M-CQD have core/shell structure. The core of the nanoparticles is Fe₃O₄ and the shells are CQDs and S-CQDs.

The elemental analysis [energy-dispersive X-ray spectroscopy (EDX)] confirms the presence of sulfur (S) atom in the as-synthesized S-M-CQDs nanoparticles (Fig. 2). On the other hand, the back titration of S-M-CQDs showed 9.6 mmol/g acidic groups (SO₃H + COOH) (Supporting Information) is loaded on the as-prepared catalyst, which is much higher than the previous published S-CDQs particles [17].

Thermal gravimetric analysis (TGA) was used to investigate the thermal stability of the as-synthesized M-CQDs, and S-M-CQDs (Fig. 3). M-CQDs losses 5% of its weight, which can be attributed to the loaded CQDs on the nano-Fe₃O₄ surface. S-M-CQDs has two main losses (region A and B), which correspond to the losses of loaded SO₃H groups and CQDs on the nano-Fe₃O₄ surface. The main loss

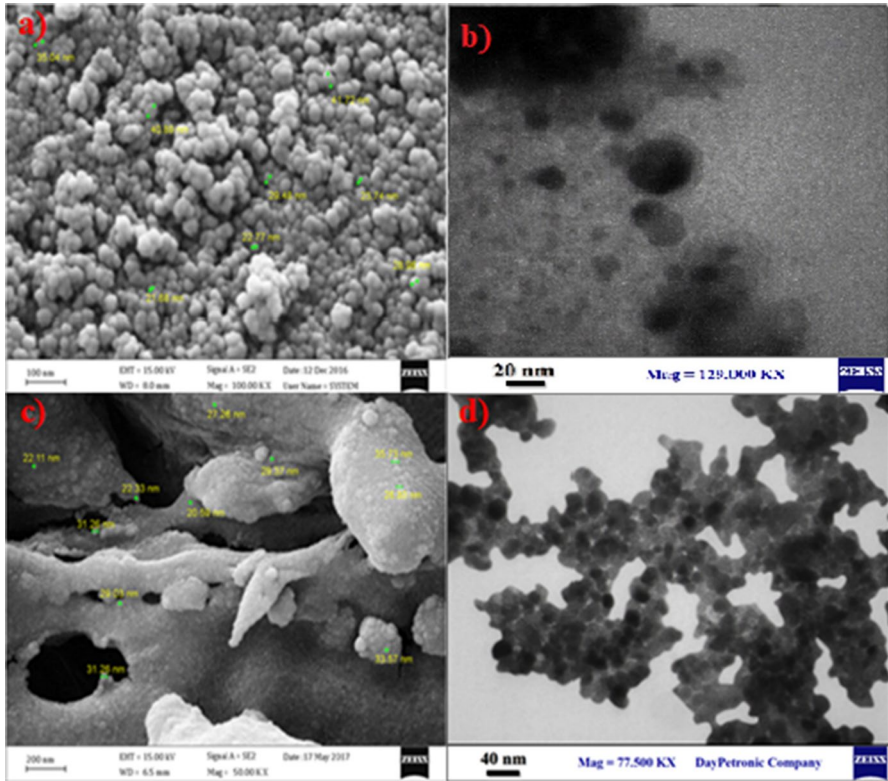


Fig. 1 Scanning electron microscopy (SEM), and transmission electron microscopy (TEM) of the M-CQDs (a, b) and S-M-CQDs (c, d)

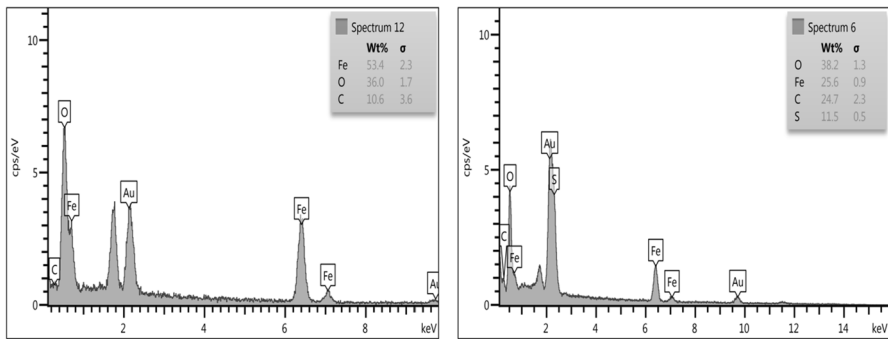


Fig. 2 The energy-dispersive X-ray spectroscopy (EDX) of M-CQDs (left) and S-M-CQDs (right) MNPs

occurs at 510 °C, which indicate thermal stability of the as-synthesized S-M-CQDs nanoparticles.

Vibrating sample magnetometer (VSM) of nano-Fe₃O₄, M-CQDs, and S-M-CQDs (Fig. 4) indicate that CQDs and S-CQDs layers on the nano-Fe₃O₄ reduce

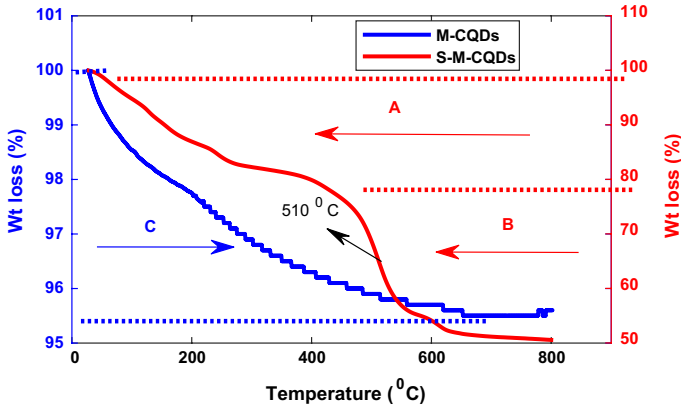


Fig. 3 The thermal gravimetric analysis (TGA) of M-CQDs, and S-M-CQDs

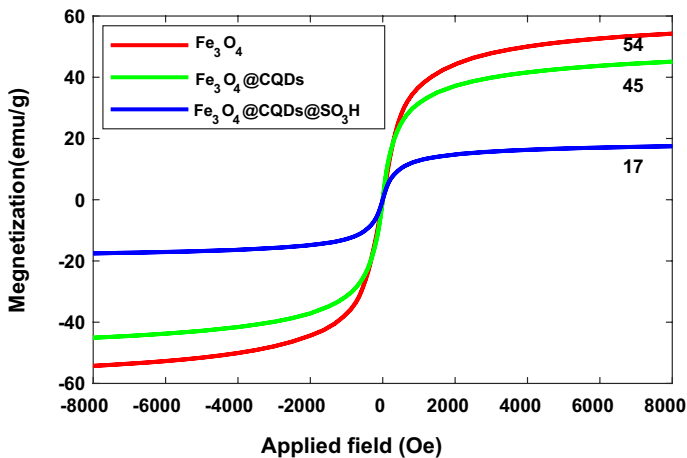


Fig. 4 Vibrating sample magnetometer (VSM) of nano- Fe_3O_4 , M-CQDs, and S-M-CQDs

the saturation magnetization of the nano- Fe_3O_4 (from 54 emu/g in nano- Fe_3O_4 to 45 emu/g, and 17 emu/g in M-CQDs and S-M-CQDs, respectively). But the magnetization is enough that M-CQDs and S-M-CQDs nanoparticles could be easily separated from reaction media using an external magnet.

To further explain the loading of CQDs on the surface of nano- Fe_3O_4 and sulfonation of hydroxyl group in the CQDs nanoparticles, the FT-IR of nano- Fe_3O_4 , M-CQDs, and S-M-CQDs were recorded (Fig. 5). The wave numbers around 3400 and 1600 cm^{-1} in M-CQDs correspond to the vibrations of O–H and C=O bonds, respectively. The peaks around 650 , 1200 , and 3400 cm^{-1} in S-M-CQDs correspond to the vibrations of S–O (stretching), S=O (asymmetric stretching), and OH groups, respectively. Therefore, we consider the changes in the surface groups of the S-M-CQDs are responsible for the photo-induced proton generation.

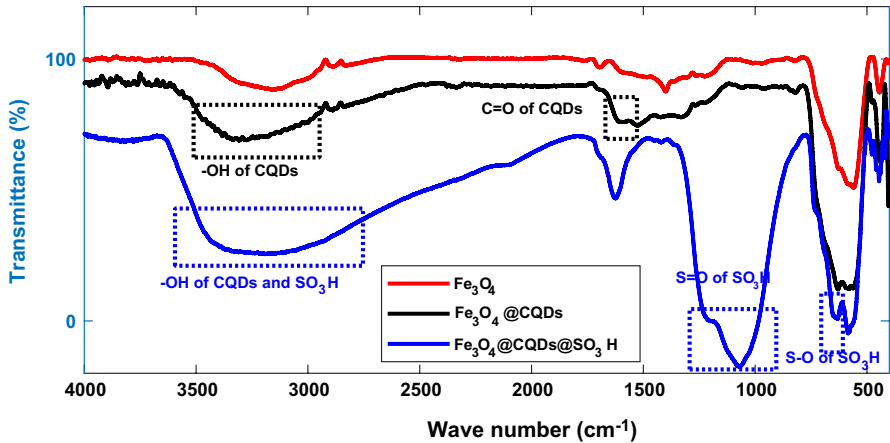


Fig. 5 Infrared Spectra (IR) of nano- Fe_3O_4 , M-CQDs, and S-M-CQDs

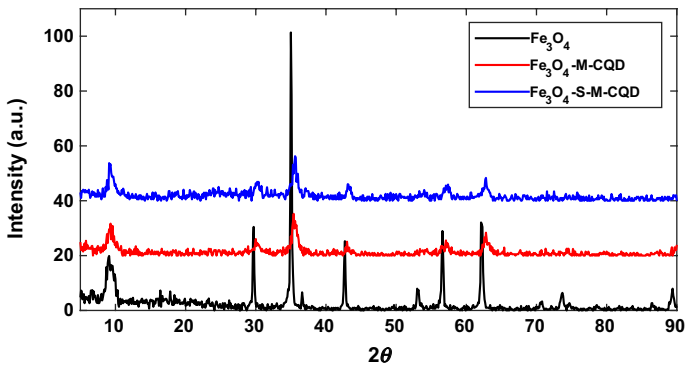
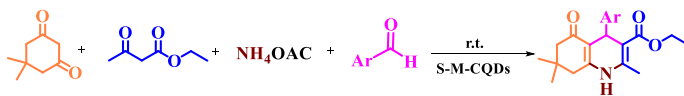


Fig. 6 XRD pattern of Fe_3O_4 , Fe_3O_4 -M-CQD, and Fe_3O_4 -S-M-CQD

The X-ray diffraction (XRD) of the nano- Fe_3O_4 , M-CQDs, and S-M-CQDs are shown in the Fig. 6. The presence of sharp peaks at XRD pattern implies the crystallinity of the as-synthesized nano-particles. The size of the magnetic nano-particles and the interplaner spacing can be determined from Sherrer's equation ($D = k\lambda/\beta\cos\theta$) and Bragg equation ($d_{hkl} = \lambda/2\sin\theta$), respectively.

Catalyst test and evaluation

Reaction between 1 mmol benzaldehyde, 1 mmol ethyl acetoacetate, 1.2 mmol ammonium acetate, and 1 mmol dimedon was used as benchmark one-pot reaction (hereafter reaction). To elucidate the photo enhanced catalytic abilities of sulfonated magnetic carbon quantum dots (S-M-CQDs), the reaction was carried out in dark, and ultra violet (UV) irradiation (at room temperature), which is shown in Table 1. To fair comparison of the reaction yield at different condition, the reaction

Table 1 Synthesis of hexahydroquinoline catalyzed by S-M-CQDs, M-CQD and other catalysts at room temperature

Entry	Yield (%) ^a		<i>t</i> (min)
	Dark	UV ^b	
1 Fe ₃ O ₄ @CQD-SO ₃ H	35	75	10
2 Fe ₃ O ₄ @CQD	21	48	10
3 p-toluene sulfonic acid	66	68	10
4 Benzoic acid	40	41	10
5 Acetic acid	46	48	10
6 Phenol	39	40	10
7 Nano Fe ₃ O ₄	31	32	10
8 Without catalyst	18	20	10

The temperature was kept constant (25 °C) using a water bath circulator

^aThe yields was obtained through crystallization method in ethyl acetate till 6 °C

^bUltraviolet irradiation at 320 nm

was ceased after 10 min. When there was no any light source (dark condition), the achieved yield is 35%. The difference in the reaction yield under the UV irradiation and dark condition is 40%, indicating that the UV irradiation has considerable effect on the reaction yield. On the other hand, the reaction was carried out using magnetic carbon quantum dots (M-CQDs), as the control reaction. After 10 min, the achieved reaction yield in the dark, and UV irradiation condition was 21%, and 48%, respectively. These results imply that S-M-CQDs is more efficient than M-CQDs. To figure out the effect of active sites (-SO₃H) on the S-M-CQDs, further control experiments in the presence of phenol, p-toluene sulfonic acid, benzoic acid, and acetic acid were carried out. Obtained reaction yield (in the dark, and UV irradiation condition) in the presence of benzoic acid, acetic acid, and phenol implies that the active site aren't hydroxyl group and carboxylic acid groups. Achieved yield in the presence of p-toluene sulfonic acid, indicate that the sulfonic acid group is the active site. In addition, the reaction was carried out in the presence of nano-Fe₃O₄, so that the obtained reaction yield (Table 1, entry 7) shows that nano-Fe₃O₄ isn't an efficient catalyst in dark, and UV irradiation condition. Lowest yield in the entry 8 shows that the catalyst has a vital role in the progression of the reaction.

To further clarify the effect of light on the M-S-CQDs (we call it M-CQD-SO₃H to explain the mechanism), pH of the water solution in dark and UV irradiation was measured. The pH value at different times is shown in Fig. 7. Water circulating bath was used to control the temperature at 25 °C, both in dark and UV irradiation. The reduced pH in the presence of UV irradiation is due to photon enhance dissociation

Fig. 7 pH value of water + M-S-CQDs solution in dark and UV irradiation

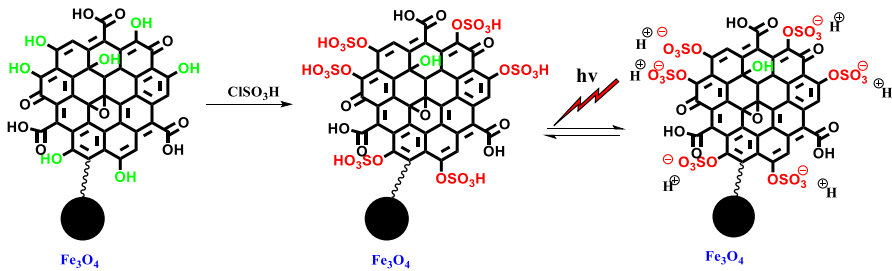
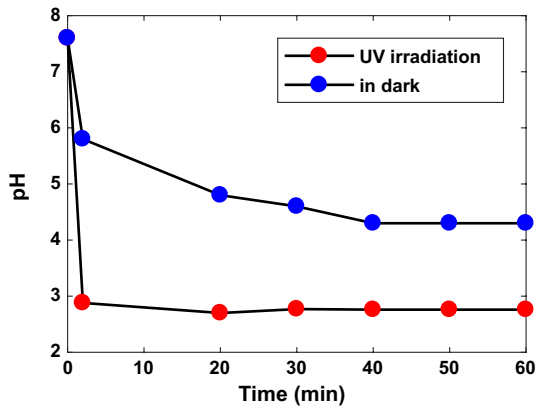


Fig. 8 The sulfonation and proposed light-induced proton generation of S-M-CQDs under light irradiation

of the M-CQD-SO₃H ($M-CQD-SO_3H + H_2O \leftrightarrow M-CQD-SO_3^- + H_3O^+$). These behaviors confirm the increase rate of the reactions in the presence of M-S-CQDs. Released H₃O⁺ activates the carbonyl group in benzaldehyde, which initiate the reaction.

Based on the above results and discussions, the proposed mechanism of photon induced proton generation under visible light and UV irradiation is shown in Fig. 8. Due to the acidic properties of the sulfonic groups, it is assumed that the light causes the generation of sulfonic protons [15].

In order to clarify the effect of light on the S-M-CQDs, the following experiments were done. Under UV irradiation, 10 experiments were carried out and the reactions ceased after 1, 2, 3, 4, 5, 6, 8, 10, 12, and 14 min, respectively. In addition, the next 5 experiments lasted for 5 min under UV condition and immediately transferred to darkness and the reactions stopped after 6, 8, 10, 12, and 14 min, respectively. To figure out the effect of sulfonic groups, the same procedure was followed by unsulfonated M-CQDs. The results are given in the Fig. 9 for M-CQDs and S-M-CQDs. The circle and square markers show the reaction yield in the presence of S-M-CQDs and M-CQDs catalyst, respectively. As is shown, after cutting off the light source, the reactions progress has stopped, which confirm the photo switchable property of

Fig. 9 Yield versus time in the presence of M-CQDs and S-M-CQDs

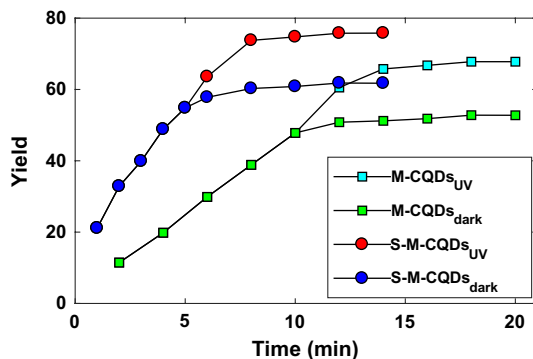
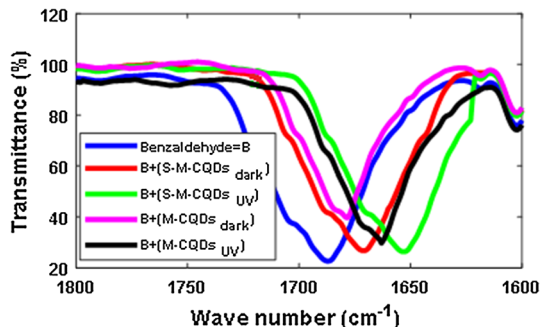
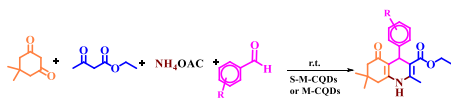


Fig. 10 FT-IR spectrum of benzaldehyde in the presence of S-M-CQDs and M-CQDs in UV and dark conditions



the as-synthesized catalysts. The separation point (5 min for S-M-CQDs and 10 min for M-CQDs) in the Fig. 9 shows that the catalyst is switchable, so that switches the conversion to on/off mode. In addition, the yield of the reaction is higher in the presence of S-M-CQDs than M-CQDs, in both UV and dark conditions, which implies dissociation of sulfonic protons. UV light enhances the reaction yield by hydrogen bonding [14] (for M-CQDs) and dissociation of sulfonic protons [15] (S-M-CQDs) mechanisms.

FT-IR technique was used to clarify the reaction yield using M-CQDs and S-M-CQDs (in UV and dark condition). It has been shown that acidic catalysts activate carbonyl bond of benzaldehyde in the benchmark reaction [18]. Accordingly, a mixture of benzaldehyde + S-M-CQDs, and benzaldehyde + M-CQDs stirred under UV and dark condition, after separation of catalysts using a magnet, the FT-IR of benzaldehyde was recorded immediately. The results are given in the Fig. 10. The frequency of carbonyl group is shifted to lower wave numbers. S-M-CQDs, which reduces carbonyl wave number from 1687 to 1653 cm^{-1} , and from 1687 to 1672 cm^{-1} at UV and dark condition, respectively. M-CQDs is less efficient than S-M-CQDs so that carbonyl wave number shift from 1687 to 1664 cm^{-1} , and from 1687 to 1679 cm^{-1} at UV and dark condition, respectively. These findings confirm the benchmark reaction yield using the as-synthesized photo switchable catalyst in UV and dark conditions. It should be noted that the M-CQDs in UV condition is more efficient than S-M-CQDs in dark condition, which is seen in both reaction yields (Fig. 9) and FT-IR spectra (Fig. 10).

Table 2 Synthesis of hexahydroquinoline derivatives catalyzed by M-CQDs, and S-M-CQD in dark and UV irradiation condition

R	UV				Dark			
	M-CQDs		S-M-CQDs		M-CQDs		S-M-CQDs	
	<i>t</i> ^a	Yield ^b	<i>t</i>	Yield	<i>t</i>	Yield	<i>t</i>	Yield
3-OMe	9	75	6	80	23	74	20	78
2,3-diCl	15	69	12	71	29	65	25	70
2-NO ₂	17	74	15	79	32	72	27	78
4-Br	12	78	9	81	21	74	20	79
3-OH	12	63	10	65	22	62	16	62
4-Me	14	68	10	75	29	53	25	82
2-F	10	83	7	86	19	80	18	85
2-Cl	8	83	6	90	20	81	18	87
3-F	15	67	11	69	26	65	20	65

^aThe time that the reaction has been completed

^bThe yield that was obtained through the crystallization in the ethyl acetate till 6 °C

To generalize the application of the photo driven property of the as synthesized catalysts, namely M-CQDs, and S-M-CQDs, different derivatives of hexahydroquinoline were synthesized in dark and UV irradiation condition. The results are given in the Table 2. As one can see, the reaction time (to complete the reaction) using the M-CQDs is higher than the S-M-CQDs for both in dark and UV irradiation condition, which shows that the $-\text{OSO}_3\text{H}$ group has vital role to promote the reaction. In addition, for all derivatives using S-M-CQDs catalyst in dark condition, the reaction times are approximately two or three times than UV irradiation condition.

Proposed catalytic mechanism

The plausible catalytic mechanism is given in the Fig. 11. The heterogeneous solid acid catalyst activates the aldehyde through $-\text{SO}_3\text{H}$ groups on the catalyst surface. Then, the enol-keto form of dimedone attacks to the activated aldehyde (intermediate 1). On the other hand, solid acid catalyst activates the carbonyl group of the ethyl acetoacetate which is attacked by ammonia (intermediate 2). Finally, the intermediate 1 and 2 react to form the final product.

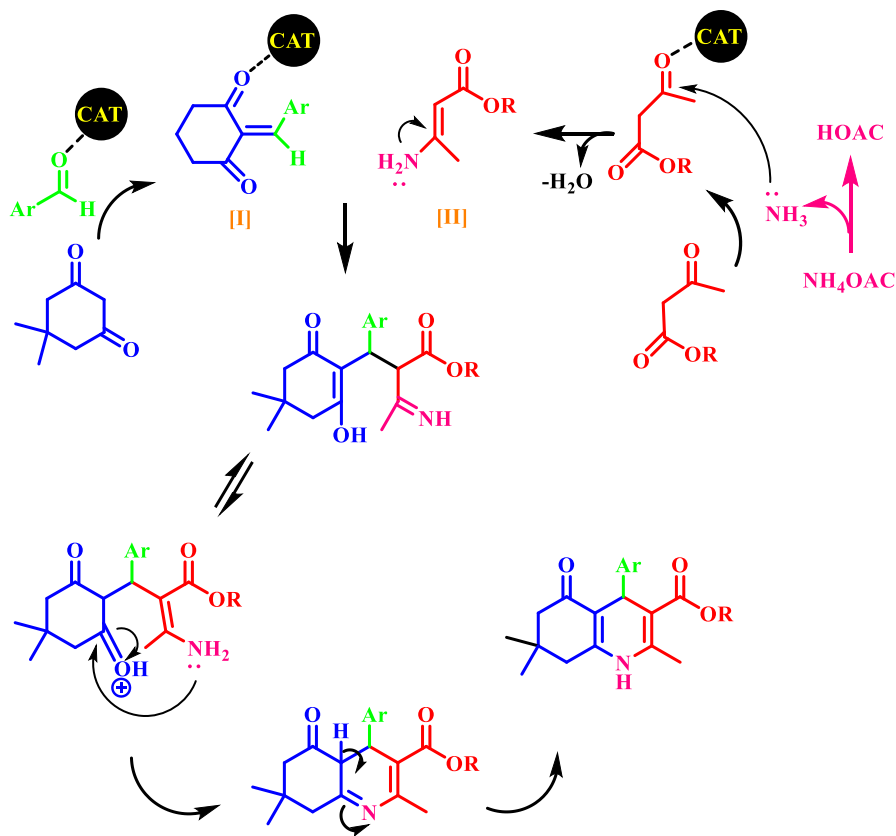


Fig. 11 The plausible catalytic mechanism in the synthesis of hexahydroquinoline derivatives

Catalyst stability

To check the catalyst stability in the one-pot reaction, the IR technique was used. Accordingly, after the catalyst preparation the IR spectrum of the catalyst was recorded. Then, after the completion of the one-pot reaction, the as-prepared catalyst was recovered and the IR spectrum was recorded. The IR spectra were identical, which imply the stability of the as-prepared catalyst in the one-pot reaction.

In the present work, the synthesized carbon quantum dots were separated using an external magnet, so that the brown water solution turned into clear water solution. This method is very economical in terms of time and cost than the dialysis method [7, 14, 17, 19]. Although sulfonated carbon quantum dots have been used for ring opening reaction [17], and carbon quantum dots for Aldol condensations [14], but separation of the carbon quantum dots is done by centrifugation (approximately 22,000–23,000 rpm) [14, 17]. Separation is not very common by this method, and the catalyst may remain in the reaction media. On the other hand, concentrated sulfuric acid (98% H₂SO₄) has been used to sulfonation of the hydroxyl group in the

carbon quantum dots [17], which is not an effective method to achieve a high density sulfonated functional group. Accordingly, in the present work, chlorosulfonic acid was used to convert $-OH$ into $-OSO_3H$ groups (SN_2 mechanism), which is a simple approach with high yield. Magnetic carbon quantum dots modified with palladium [15], and magnetic core-shell carbon dots@MFe₂O₄ with application in Suzuki reaction and reduction of p-nitrophenol [18], respectively, have been reported. Use of carbon quantum dots as catalyst in organic chemistry is in the early stages and needs more research, so that in this work magnetic carbon quantum dots was used in the synthesis of hexahydroquinoline derivatives as a representative of multicomponent one-pot reactions.

Conclusion

In summary, we demonstrated that separation of CQDs can be easily achieved through magnetic Fe₃O₄ than ultracentrifugation and dialysis methods. Anchoring high density stronger acid groups such as $-OSO_3H$ on the surface of magnetic CQDs can be obtained using chlorosulfonic acid. Magnetic CQDs (M-CQDs) and sulfonated S-M-CQDs was synthesized and photo proton generation property of S-M-CQDs was shown. The preparation of photo enhanced and switchable (on/off mode) sulfonated magnetic carbon quantum dots is described and used in the one-pot multicomponent reaction at room temperature. Hope these findings motivate researchers to develop more photo responsive catalysts in organic chemistry.

Acknowledgements The authors gratefully acknowledge the Bu-Ali Sina University Research Council and Center of Excellence in Development of Environmentally Friendly Methods for Chemical Synthesis (CEDEFMCS), Iran National Science Foundation (INSF) for providing support to this work. This work was supported by Key Laboratory of Advanced Control and Optimization for Chemical Processes (CN) (Grant No. 32-1716).

References

1. H.W. Kroto, J.R. Heath, S.C. Orien, R.F. Curl, R.E. Smalley, *Nature* **318**, 6042 (1985)
2. W. Kratschmer, L.D. Lamb, K. Fostiropoulos, D.R. Huffman, *Nature* **347**, 6291 (1990)
3. S. Iijima, *Nature* **354**, 6348 (1991)
4. S. Iijima, T. Ichihashi, *Nature* **363**, 6430 (1993)
5. K.S. Novoselov, A.K. Geim, S.V. Morozov, D. Jiang, Y. Zhang, S.V. Dubonos, I.V. Grigorieva, A.A. Firsov, *Science* **306**, 5696 (2004)
6. L.A. Ponomarenko, F. Schedin, M.I. Katsnelson, R. Yang, E.W. Hill, K.S. Novoselov, A.K. Geim, *Science* **320**, 5874 (2008)
7. X. Xu, R. Ray, Y. Gu, H.J. Ploehn, L. Gearheart, K. Raker, W.A. Scrivens, *J. Am. Chem. Soc.* **126**, 40 (2004)
8. H. Li, Z. Kang, Y. Liu, S.-T. Lee, *J. Mater. Chem.* **22**, 46 (2012)
9. L. Cao, X. Wang, M.J. Mezirani, F. Lu, H. Wang, P.G. Luo, Y. Lin, B.A. Harruff, L.M. Veca, D. Murray, S.-Y. Xie, Y.-P. Sun, *J. Am. Chem. Soc.* **129**, 37 (2007)
10. H. Jiang, F. Chen, M.G. Lagally, F.S. Denes, *Langmuir* **26**, 3 (2010)
11. V. Georgakilas, J.A. Perman, J. Tucek, R. Zboril, *Chem. Rev.* **115**, 11 (2015)
12. H. Liu, T. Ye, C. Mao, *Angew. Chem. Int. Ed.* **46**, 34 (2007)
13. S.Y. Lim, W. Shen, Z. Gao, *Chem. Soc. Rev.* **44**, 1 (2015)

14. Y. Han, H. Huang, H. Zhang, Y. Liu, X. Han, R. Liu, H. Li, Z. Kang, *ACS Catal.* **4**, 3 (2014)
15. H. Li, R. Liu, W. Kong, J. Liu, Y. Liu, L. Zhou, X. Zhang, S.-T. Lee, Z. Kang, *Nanoscale* **6**, 2 (2014)
16. B. Majumdar, S. Mandani, T. Bhattacharya, D. Sarma, T.K. Sarma, *J. Org. Chem.* **82**, 4 (2017)
17. H. Li, C. Sun, M. Ali, F. Zhou, X. Zhang, D.R. MacFarlane, *Angew. Chem. Int. Ed.* **54**, 29 (2015)
18. A. Khazaei, N. Sarmasti, J.Y. Seyf, M. Tavasoli, *RSC Adv.* **5**, 123 (2015)
19. Z. Zhang, T. Zheng, X. Li, J. Xu, H. Zeng, *Part. Part. Syst. Character.* **33**, 8 (2016)

Publisher's Note Springer Nature remains neutral with regard to jurisdictional claims in published maps and institutional affiliations.